

**FULL PAPER****Applied
Organometallic
Chemistry****WILEY**

Preparation and characterization of Cu supported on 2-(1*H*-benzo[*d*]imidazol-2-yl)aniline-functionalized Fe₃O₄ nanoparticles as a novel magnetic catalyst for Ullmann and Suzuki cross-coupling reactions

Liang Danqing¹ | Jin Ming¹ | Li Li² | Majid Mohammadnia³

¹Department of Institute of Physical Education, Shijiazhuang University, Shijiazhuang, China

²Department of Mechanical and Electrical College, Shijiazhuang University, Shijiazhuang, China

³Young Researcher and Elite Club, Department of Chemistry, Bojnord Branch, Islamic Azad University, Bojnourd, Iran

Correspondence

Liang Danqing, Department of Institute of Physical Education, Shijiazhuang University, Shijiazhuang, China.
Email: zhanghap85@163.com

Copper supported on 2-(1*H*-benzo[*d*]imidazol-2-yl)aniline (BIA)-functionalized Fe₃O₄ nanoparticles (Cu-BIA-Si-Fe₃O₄) as a novel magnetic catalyst was designed and used for the synthesis of new products via Ullmann and Suzuki cross-coupling reactions. The Ullmann reaction was performed by mixing arylboronic acid with aniline derivatives in dimethylsulfoxide solvent. Also, diaryls were synthesized via Suzuki C–C reactions between aryl halides and phenylboronic acid in the same solvent. The prepared materials and catalyst were characterized with various analytical techniques. The Cu-BIA-Si-Fe₃O₄ catalyst demonstrated catalytic efficiency with good to excellent yields for both types of reactions in comparison with commercial palladium catalysts. Also, the catalyst could be recovered by a simple filtration and retained its activity even after several cycles.

KEY WORDS

coupling reaction, Cu nanoparticles, Schiff base, Suzuki reaction, Ullmann reaction

1 | INTRODUCTION

In recent years, with the development of nanotechnology, nanomaterial-based catalysts have been used as important heterogeneous catalysts in the synthesis of various organic compounds.^[1,2] One of these nanomaterials are magnetic nanoparticles (MNPs) with exceptional characteristics such as good eco-friendliness and biodegradability, efficiency, easy accessibility, low or no toxicity and high specific surface area for increasing catalyst loading capacity and noticeable sustainability of heterogeneous supports for preparation of various catalysts.^[3,4] These characteristics of MNPs comfortably cause them to be good, enhanced catalyst candidates.^[5] Appropriate surface modification of MNPs is vital to make them biocompatible and biodegradable. Generally, the coating method is the most common surface modification approach for

conjugating organic or inorganic materials onto the surface of MNPs. All of these constructed catalysts can be quickly separated using an external magnet and recycled.^[6,7]

These days, transition metal-catalyzed cross-coupling reactions have become an important and well-known method for the formation of C–C, C–N and C–S bonds via combination of electrophilic and nucleophilic segments. In fact, the construction of C–C, C–N and C–S bonds is vital for the preparation of a diversity of biologically active and organic compounds.^[8] The formation of C–N bond is an important key reaction having wide applications in the synthesis of organic functional molecules. Usually, C–N bonds are constructed using copper- and palladium-catalyzed amination of aryl halides as well as arylboronic acids.^[9] Transition metal-mediated C–N bond formation is a fundamental

transformation that allows the preparation of noteworthy amine products like diarylamines or diphenylamines via coupling reactions.^[10,11] Also, to form C&—C bonds in biaryl or diphenyl compounds, the most significant procedure is through transition metal-catalyzed Suzuki cross-coupling reactions between an aryl electrophile and aryl nucleophile or aryl halides and phenylboronic acid.^[12]

Diaryls are a valuable class of organic compounds with wide applicability in the polymer and life science industries as well the chemical industry.^[13,14] A number of them display substantial special biological and pharmacological activities.^[15–17] Due to their significance, development of efficient methods for their synthesis is still a challenging and active area of research and they have captured the interests of researchers for a long time. Among the various protocols reported to date, those involving copper-based catalysts are the most general pathways for the generation of these compounds. Common ways to synthesize these compounds are via Pd- or Cu-catalyzed Ullmann coupling and Suzuki cross-coupling.^[18–20] Among Pd- or Cu-catalyzed Ullmann reactions, Pd-catalyzed C&—C and C&—N bond formations are prospering to certain expanse and Cu-based catalysts are more favorable because of cheap raw materials, simple and easy performances and low toxicity.^[21,22]

Also, Pd- or Cu-catalyzed Ullmann and Suzuki reactions are generally carried out with high catalyst loadings^[23] or need high temperatures^[24] which prevent their application for the preparation of complex molecules.^[17,25] Many researchers have demonstrated that specific additives, which certainly operate as copper ligands, improve reaction rates and allow the couplings to be performed at more moderate temperatures, in the presence of decreased amounts of copper or with a larger substrate area. Recently, many new and unique ligands have appeared and been introduced such as 1,10-phenanthroline and its derivatives,^[26] ethylene glycol,^[27] N,N-dimethylglycine,^[28] diethylsalicylamide, oxime-type and Schiff base ligands,^[29] amino acids,^[30] thiophene-2-carboxylate,^[31] aminoarenethiolate,^[32] ethylene glycol diacetate,^[33] bidentate phosphines,^[34] phosphine ligands,^[35] (S)-2,2,6,6-tetramethylheptane-3,5-dione,^[36] 2-aminopyrimidine-4,6-diol,^[37] phosphazene P4-tBu base^[38] and so on.

Despite remarkable developments in the heterogeneous recoverable copper-catalyzed Ullmann reaction, these days the reusability of the catalyst support is attracting much attention. Hence, application of an efficient alternative to conventional heterogeneous catalyst supports like functionalized MNPs with a range of chemical materials including types of metal complexes,

functional groups and metal nanoparticles (e.g. Pd, Si or Cu) is significant.^[39]

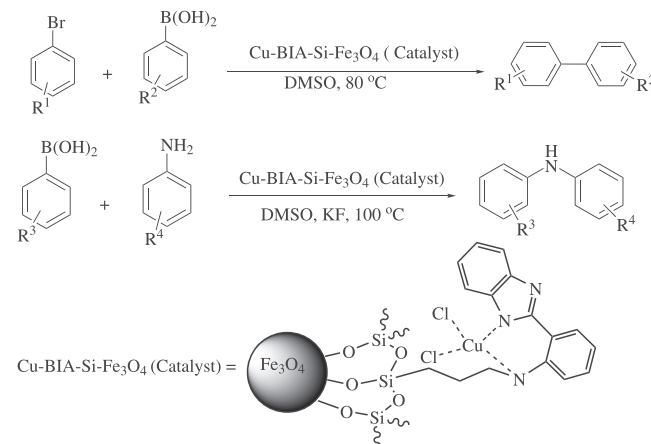
In the work reported here, first was constructed a new, efficient, biodegradable and biocompatible heterogeneous recoverable functionalized catalyst consisting of Cu supported on 2-(1*H*-benzo[*d*]imidazol-2-yl)aniline (BIA)-functionalized Fe₃O₄ magnetic nanoparticles (Cu-BIA-Si-Fe₃O₄). Then, the prepared catalyst was employed for Suzuki coupling reactions between aryl halides and phenylboronic acid and Ullmann coupling reactions between arylboronic acid and anilines (Scheme 1). The Cu-BIA-Si-Fe₃O₄ catalyst was characterized using various techniques such as Fourier transform infrared (FT-IR) spectroscopy, X-ray diffraction (XRD), scanning electron microscopy (SEM), transmission electron microscopy (TEM), thermogravimetric analysis (TGA), vibrating sample magnetometry (VSM), energy-dispersive X-ray (EDX) analysis and inductively coupled plasma atomic emission spectrometry (ICP-AES) (Scheme 1).

2 | RESULTS AND DISCUSSION

2.1 | Characterization of prepared Cu-BIA-Si-Fe₃O₄ MNPs

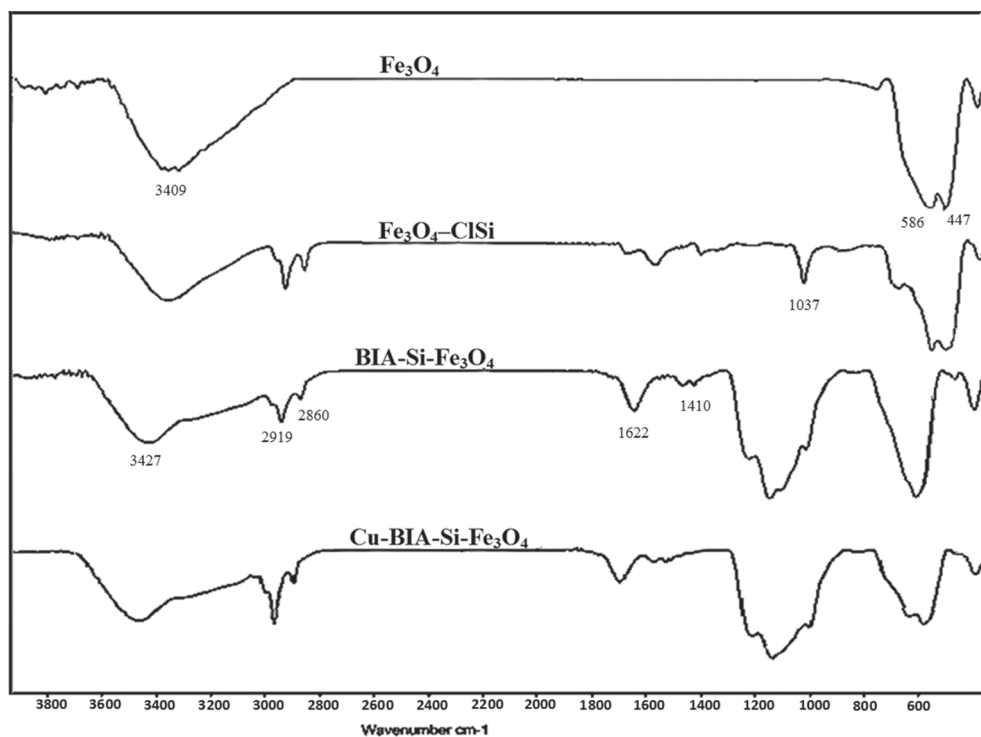
2.1.1 | FT-IR spectroscopic analysis

The FT-IR spectra of Fe₃O₄, Fe₃O₄-ClSi, BIA-Si-Fe₃O₄ and Cu-BIA-Si-Fe₃O₄ are illustrated in Figure 1. The bands at 586 and 447 cm⁻¹ were attributed to Fe&—O stretching and that at 3409 cm⁻¹ corresponded to OH groups on the magnetic surface of MNPs. Also, in the FT-IR spectrum of Fe₃O₄-ClSi, the absorption band at 1037 cm⁻¹ is assigned to the Si&—O groups. In the FT-IR



S C H E M E 1 Ullmann and Suzuki cross-coupling reactions catalyzed by Cu-BIA-Si-Fe₃O₄

FIGURE 1 FT-IR spectra of Fe_3O_4 , $\text{Fe}_3\text{O}_4-\text{ClSi}$, BIA-Si- Fe_3O_4 and Cu-BIA-Si- Fe_3O_4



spectrum of BIA-Si- Fe_3O_4 , new bands were observed at 1622 and 1410 cm^{-1} assigned to the C&d=D and C&—H (aromatic) stretching vibrations, respectively. The characteristic bands at 2860 and 2919 cm^{-1} are assigned to the symmetric and asymmetric stretching of C&—H bonds in 1*H*-benzo[*d*]imidazol-2-amine and propyl group unit of BIA-Si- Fe_3O_4 MNPs. These bands confirmed that 1*H*-benzo[*d*]imidazol-2-amine had been successfully reacted with amino present in the structure of BIA-Si- Fe_3O_4 . The N&—H stretching peak of the amide group in BIA-Si- Fe_3O_4 appeared at 3427 cm^{-1} . In addition, in the FT-IR spectrum of Cu-BIA-Si- Fe_3O_4 , the intensity of the adsorption band at 629 cm^{-1} that is assigned to the bending vibration of C&—H in pyridine heterocyclic ring is reduced after formation of BIA-Si- Fe_3O_4 complex with Cu. Therefore, the data obtained from FT-IR spectroscopy can indicate the existence of the nanomagnetic particles, heterocyclic moiety and Cu in the structure of Cu-BIA-Si- Fe_3O_4 MNPs (Figure 1).

2.1.2 | XRD analysis

XRD is employed as an experimental method for determining the atomic and molecular structure of a crystal, in which the crystalline structure causes a beam of incident X-ray to diffract in many special directions.^[34] The powder XRD patterns of two samples, Fe_3O_4 nanoparticles and Cu-BIA-Si- Fe_3O_4 nanoparticles, are

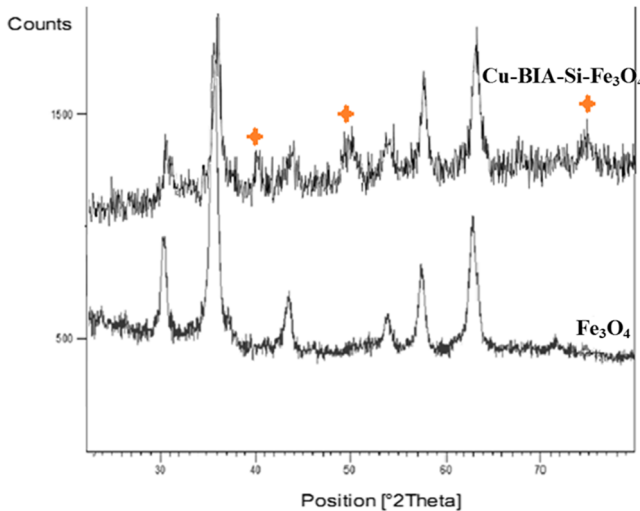


FIGURE 2 XRD patterns of Fe_3O_4 nanoparticles and Cu-BIA-Si- Fe_3O_4 nanoparticles

displayed in Figure 2. It can be seen that the Fe_3O_4 obtained has a highly crystalline cubic spinel structure which agrees with the standard Fe_3O_4 (cubic phase) XRD pattern (PDF no. 88-0866). The patterns indicate a crystalline structure with peaks at $2\theta = 30.2^\circ$, 35.30° , 43.3° , 53.65° , 57.3° and 62.8° corresponding to (220), (311), (400), (422), (511) and (440), indicative of the cubic spinel structure of Fe_3O_4 MNPs. Also, in the XRD pattern of Cu-BIA-Si- Fe_3O_4 nanoparticles (Figure 2), the peaks at $2\theta = 42.87^\circ$, 50.26° and 74.56° are assigned to (111), (200), (220), (220), (311), (400), (422), (511) and (440),

indicative of the cubic spinel structure of Cu-BIA-Si- Fe_3O_4 .^[40] Hence, according to the results obtained from XRD analysis, one can confirm the presence of Cu on organic group moiety in the Cu-BIA-Si- Fe_3O_4 nanoparticles. The average Fe_3O_4 and Cu-BIA-Si- Fe_3O_4 core diameters were calculated to be about 10 and 11.5 nm from the XRD results using Scherrer's equation, $D = k\lambda/\beta \cos \theta$, where k is a constant (generally considered as 0.94), λ is the wavelength of Cu K α (1.54 Å), β is the corrected diffraction line full width at half-maximum and θ is Bragg's angle.

2.1.3 | EDX analysis

The EDX analysis of Cu-BIA-Si- Fe_3O_4 is shown in Figure 3. As can be seen, Cu-BIA-Si- Fe_3O_4 is composed of the expected elements in the structure of the catalyst including C, O, N, Fe, Cu and Cl, indicating that Cu has been correctly grafted to BIA-Si- Fe_3O_4 .

2.1.4 | ICP-AES analysis

ICP-AES analysis was used to indicate the same Cu concentration on the Cu-BIA-Si- Fe_3O_4 as catalyst. In addition, the absence of palladium metal in the reaction solvent demonstrated no metal leaching into the reaction mixture. ICP-AES analysis indicated the weight percentage of Cu to be 10% in Cu-BIA-Si- Fe_3O_4 MNPs.

2.1.5 | Thermogravimetric analysis

Information about the loading of Fe_3O_4 nanoparticles with organic groups was obtained using TGA. The results

revealed that the Cu-BIA-Si- Fe_3O_4 nanoparticles contain about 13.62% of organic material (volatile components disappearing up to a temperature of about 100°C were neglected) (Figure 4). The composition ratio of the catalyst can be evaluated from the residual mass percentage. As exhibited in Figure 4, the first weight loss stage at almost 120°C (0.42%) was assigned to the evaporation of adsorbed water molecules. The second weight loss at 120–330°C (5.77%) can be attributed to loss of 1H-benzo[d]imidazol-2-amine group. The final weight loss at 330–600°C (7.85%) was attributed to propyl group. According to the obtained results, the good connecting of Cu-BIA-Si on the Fe_3O_4 nanoparticles is asserted. The amount of adsorbed organic compounds calculated using Equation 1 is 0.5 mmol g⁻¹:

$$\text{Organic compounds (mmol)} \quad (1)$$

$$= (\text{weight loss}/100 \times \text{Mw organic compounds}) \times 1000$$

$$= 0.5 \text{ mmol}$$

2.1.6 | TEM analysis

Morphologies of the synthesized Cu-BIA-Si- Fe_3O_4 nanoparticles were investigated using TEM as shown in Figure 5. Particles are observed to have a spherical morphology. Average particle size is estimated at about 14 nm from the TEM micrographs, which is in very good agreement with the crystallite size estimated from XRD at 11.5 nm. As shown in Figure 5, a basically core-shell structure (dark-colored core for Fe_3O_4 nanoparticles and light-colored shell for organic group) was obtained. This is an indication of nearly single crystalline character of the Cu-BIA-Si- Fe_3O_4 nanoparticles.

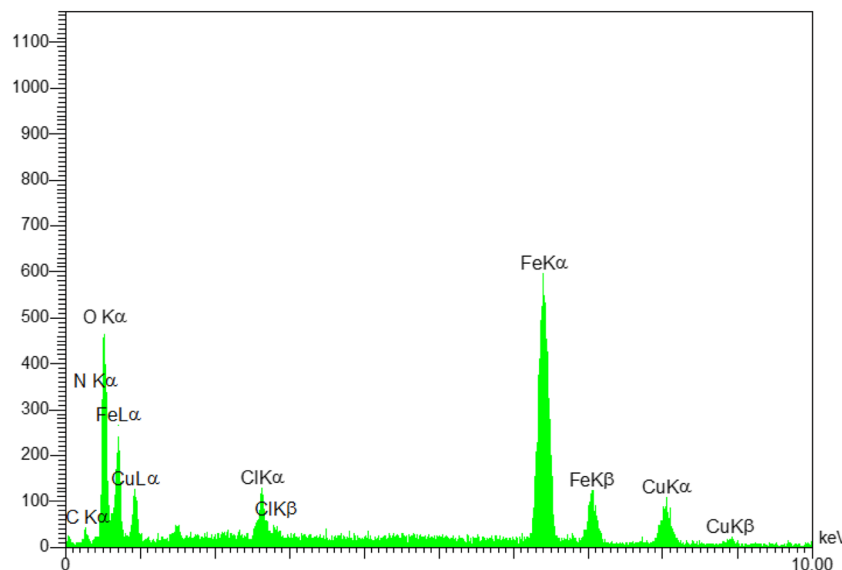


FIGURE 3 EDX spectrum of Cu-BIA-Si- Fe_3O_4

FIGURE 4 TGA diagram of Cu-BIA-Si- Fe_3O_4

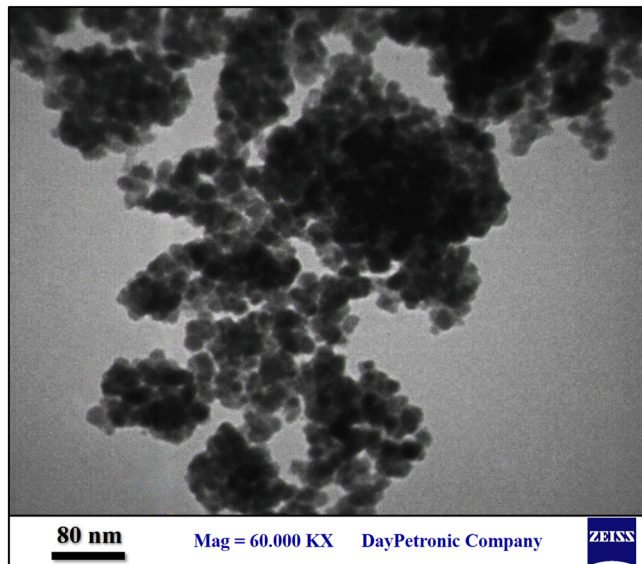
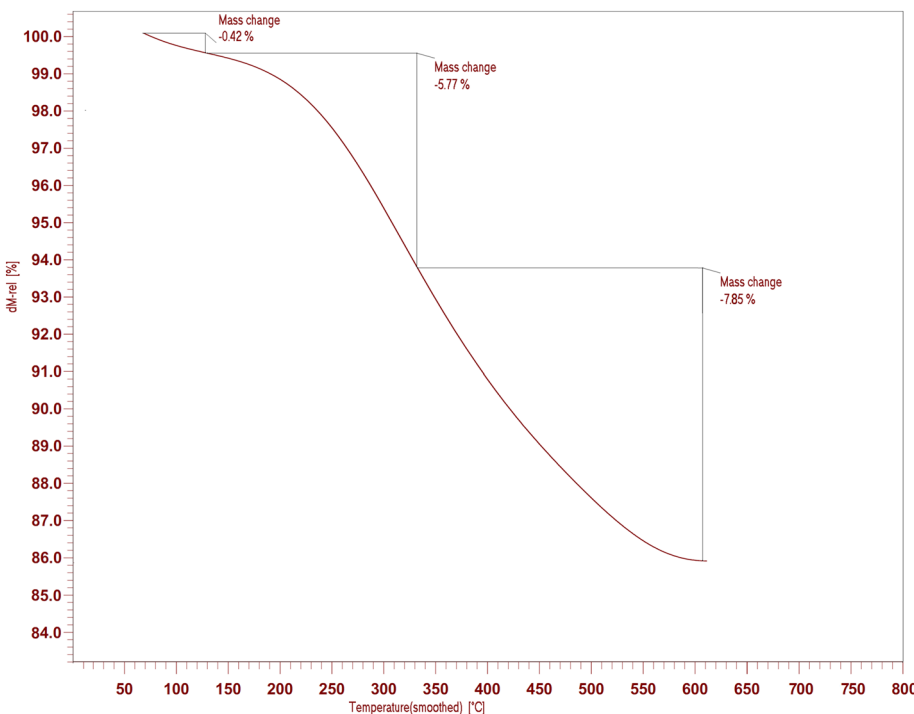


FIGURE 5 TEM micrograph of Cu-BIA-Si- Fe_3O_4 nanoparticles

2.1.7 | SEM analysis

SEM is a primary tool for determining the size distribution, particle shape, surface morphology and fundamental physical properties. An SEM image of the Cu-BIA-Si- Fe_3O_4 nanoparticles is shown in Figure 6. The SEM image of Cu-BIA-Si- Fe_3O_4 displayed a sphere like structure. It was seen to have individual crystallite sizes in the range of 20 nm.

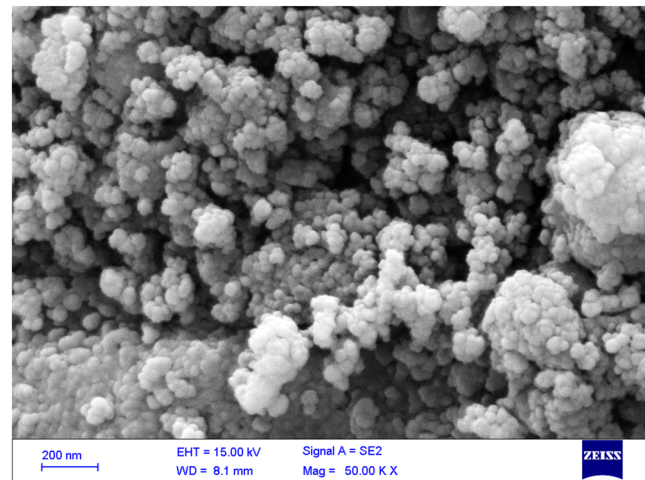


FIGURE 6 SEM image of Cu-BIA-Si- Fe_3O_4 nanoparticles

2.1.8 | Magnetic properties of catalyst

VSM was used for characterizing the magnetic properties of Fe_3O_4 , $\text{Fe}_3\text{O}_4-\text{ClSi}$, BIA-Si- Fe_3O_4 and Cu-BIA-Si- Fe_3O_4 at 300 K (Figure 7). The magnetization curves for these nanoparticles show no hysteresis in their magnetizations. As can be seen in Figure 7, the saturation magnetization values for Fe_3O_4 , $\text{Fe}_3\text{O}_4-\text{ClSi}$, BIA-Si- Fe_3O_4 and Cu-BIA-Si- Fe_3O_4 were 73.8, 62.2, 58.7 and 48.6 emu g⁻¹, respectively. A small decrease of the saturation magnetization of Cu-BIA-Si- Fe_3O_4 was observed because of the grafting of Cu on the surface of BIA-Si- Fe_3O_4 nanoparticles. In other words, the differences in magnetization are due to

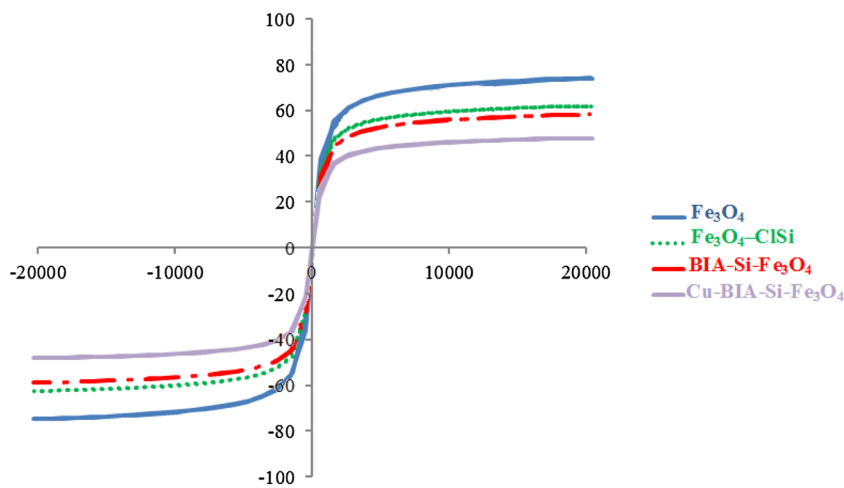


FIGURE 7 Room temperature magnetization curves of Fe_3O_4 , $\text{Fe}_3\text{O}_4\text{-ClSi}$, BIA-Si- Fe_3O_4 and Cu-BIA-Si- Fe_3O_4

the different coating layers and their thicknesses on the surface of MNPs. In any case, the prepared magnetic catalyst has excellent magnetic characteristics and can be easily separated from reaction media completely using an external magnetic field.

2.2 | Catalytic application of Cu-BIA-Si- Fe_3O_4 nanoparticles

To find optimum conditions, the reaction of aryl halide and phenylboronic acid for the synthesis of diaryl in the presence of Cu-BIA-Si- Fe_3O_4 as novel catalyst was used as a model reaction. The reaction was carried out with

different amounts of the catalyst (0.5, 1, 1.5 and 2 mol%) at several temperatures with various solvents. As evident from Table 1, the optimized reaction conditions are the use of Cu-BIA-Si- Fe_3O_4 (1.5 mol%) using 1 mmol of K_2CO_3 as the base at 80°C in DMSO (4 ml).

Next, to prepare diaryls, Suzuki cross-coupling reactions of aryl halide derivatives and phenylboronic acid derivatives under optimum conditions were used. A wide range of substituted and structurally diverse aryl halides and phenylboronic acids were employed and the corresponding products were prepared in good to excellent yields (Table 2).

The proposed mechanism for the coupling of aryl halides and boronic acids is depicted in Scheme 2. The

TABLE 1 Optimization of conditions for preparation of biphenyl in the presence of different amounts of Cu-BIA-Si- Fe_3O_4 as catalyst using 1 mmol of K_2CO_3 as base at various temperatures

Entry	Solvent	Amount of catalyst (mol%)	Temperature (°C)	Time (h)	Yield (%) ^[a]	TON	TOF (h ⁻¹)
1	CH ₃ CN	1	70	10	70	70	7
2	DMF	1	110	4	75	75	18.75
3	DMSO	1	100	2	80	80	40
4	CH ₃ OH	1	60	10	65	65	6.5
5	H ₂ O	1	100	12	40	40	3.33
6	DMSO	0.5	50	4	—	—	—
7	DMSO	1	50	4	Trace	—	—
8	DMSO	1.5	50	4	Trace	—	—
9	DMSO	2	50	4	28	14	3.5
10	DMSO	0.5	80	3	46	92	30.66
11	DMSO	1	80	3	51	51	17
12	DMSO	1.5	80	2	95	63.3	31.65
13	DMSO	2	80	2	96	48	24
14	No catalyst	—	100	24	No reaction	—	—
15	CuCl ₂ -DMSO	2	80	4	70	35	8.75

^aYields refer to isolated products.

TABLE 2 One-pot reactions of diaryl derivatives using Cu-BIA-Si-Fe₃O₄ as nanomagnetic catalyst

Entry	Aryl halide	Phenylboronic acid	Product	Time (h)	Yield	TON	TOF (h ⁻¹)	Melting point (°C)	
								Found	Reported
1	Br-C ₆ H ₄ -OCH ₃	B(OH) ₂	C ₆ H ₄ -OCH ₃	2	95	63.3	31.65	89–90	87–88 [41]
2	Br-C ₆ H ₄ -OCH ₃	H ₃ CO-C ₆ H ₄ -B(OH) ₂	H ₃ CO-C ₆ H ₄ -B(OH) ₂ -OCH ₃	2	97	64.6	32.3	173	172–174 [42]
3	Br-C ₆ H ₄ -OCH ₃	C ₂ H ₅ -C ₆ H ₄ -B(OH) ₂	C ₂ H ₅ -C ₆ H ₄ -B(OH) ₂ -OCH ₃	3	91	60.6	20.2	222	221–224 [43]
4	Br-C ₆ H ₄ -CN	H ₃ CO-C ₆ H ₄ -B(OH) ₂	H ₃ CO-C ₆ H ₄ -B(OH) ₂ -CN	3	92	61.3	20.4	100	99.4–101.4 [44]
5	Br-C ₆ H ₄ -CN	C ₂ H ₅ -C ₆ H ₄ -B(OH) ₂	C ₂ H ₅ -C ₆ H ₄ -B(OH) ₂ -CN	2	84	56	28	189–190	188–190 [45]
6	Br-C ₆ H ₄	C ₂ H ₅ -C ₆ H ₄ -B(OH) ₂	C ₂ H ₅ -C ₆ H ₄ -B(OH) ₂ -C ₆ H ₅	3	90	60	20	210–211	211–213 [46]
7	Br-C ₆ H ₄ -NO ₂	B(OH) ₂	C ₆ H ₄ -B(OH) ₂ -NO ₂	2.5	90	60	24	59–60	57–58 [47]

(Continues)

TABLE 2 (Continued)

Entry	Aryl halide	Phenylboronic acid	Product	Time (h)	Yield	TON	TOF (h ⁻¹)	Melting point (°C)	
								Found	Reported
8				3	95	63	21	71–72	70–72 [46]
9				3	93	62	20.6	69–70	70–72 [46]
10				3	93	62	20.6	71	70–72 [46]
11				2.5	90	60	24	87–89	87–88 [41]
12				3	91	60.6	20.2	89	87–88 [41]
13				2.5	94	62.6	25	99–100	99.4–101.4 [44]
14				2.5	93	62	24.8	98–100	99.4–101.4 [44]

TON: turnover number, yield of product/mol of Cu).
 TOF: turnover frequency, TON/time of reaction.

reaction is initiated by nucleophilic coordination of amine with Cu(II) of the Cu-BIA-Si-Fe₃O₄ catalyst resulting in (A), which undergoes transmetalation with boronic acid to furnish coupled Cu(II) complex (B). Oxidation of (B) in turn affords complex (C) involving Cu as Cu(III). Complex (C) on reductive elimination furnishes the final C&—C coupled product (D) and regenerates the Cu(I) catalyst which is further oxidized to Cu(II) in the presence of air. There is an added advantage of the magnetically separable heterogeneous catalyst in that it can be easily recovered after completion of the reaction without any significant loss (Scheme 2).

The most significant advantage of a heterogeneous solid catalyst in organic reactions is its recoverability and reusability. Hence, the recoverability and reusability of the catalyst were studied using the selected model reaction of aryl bromide and phenylboronic acid in DMSO (Table 2, entry 1). The reaction mixture was cooled to room temperature when the reaction was completed. After that, the catalyst was recovered using a magnetic field, washed with deionized water and ethanol, and dried for the next run. According to the results, the catalyst has good activity, reusability and stability in the reaction media and can be reused five times without any loss of its activity (Figure 8).

In order to compare the catalyst of the present work with several results reported in the literature, some of the results for the preparation of diaryls are summarized in Table 3. The obtained results indicated that Cu-BIA-Si-Fe₃O₄ is a better catalyst because of the short reaction times and good yields of products.

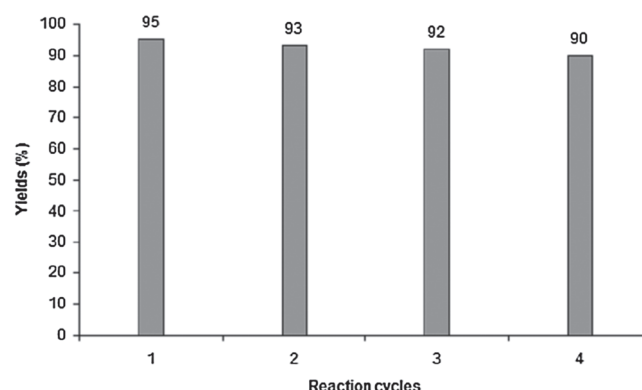
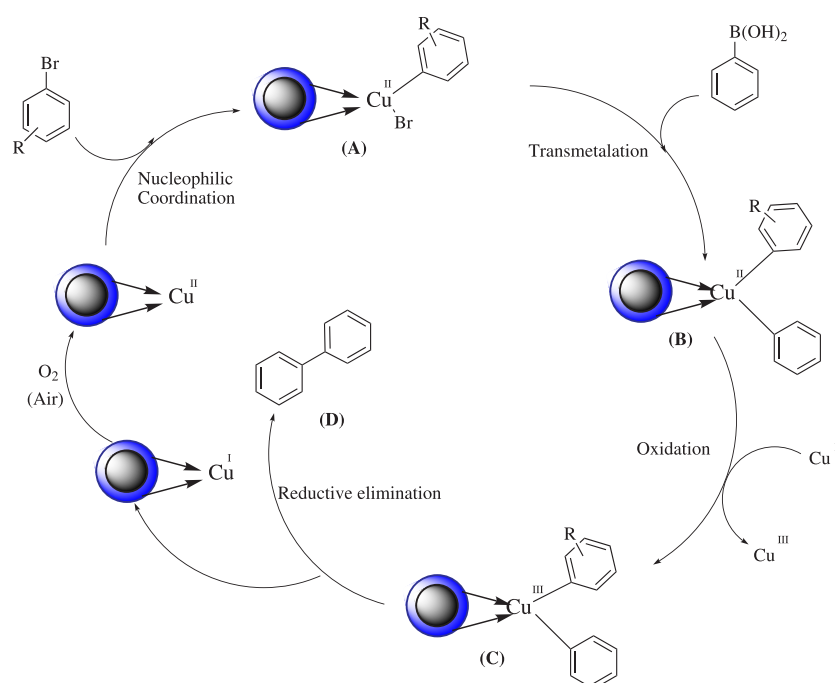


FIGURE 8 Recycling of Cu-BIA-Si-Fe₃O₄ for preparation of diaryls

Encouraged by the satisfactory results for the synthesis of diaryls, we decided to broaden the study of the catalytic activity of Cu-BIA-Si-Fe₃O₄ in the synthesis of diphenylamine derivatives. The reaction conditions were optimized starting from aniline (1 mmol) and phenylboronic acid (1.2 mmol) catalyzed by various amounts of the catalyst (0.5, 1, 1.5 and 2 mol%) with various temperatures and solvents. As a result, the optimized reaction conditions for the reaction of aniline and phenylboronic acid are the use of Cu-BIA-Si-Fe₃O₄ (1.5 mol%) and KF (0.2 mmol) in DMSO (4 ml) at 100°C (Table 4).

The applicability of the prepared catalyst in the synthesis of diarylamines was studied under the optimum reaction conditions. The reported results in Table 5 indicate that anilines and phenylboronic acid derivatives



SCHEME 2 Suggested mechanism for synthesis of diaryls via Suzuki C&—C reactions in presence of Cu-BIA-Si-Fe₃O₄ nanocatalyst

TABLE 3 Comparison of Cu-BIA-Si-Fe₃O₄ with other catalysts in Suzuki reaction for synthesis of diaryls

Entry	Catalyst	Conditions	Time (h)	Yield (%) ^[a]
1	Palladium <i>N</i> -heterocyclic carbene (0.02 mmol), K ₂ CO ₃ (1.2 eq)	i-PrOH (4 ml), r.t.	6	98 ^[48]
2	Pd(OAc) ₂ /LHX (15 mol%)	DMF/H ₂ O (2 mmol), 50°C	3	93 ^[49]
3	Aminomethylidiphosphine-Pd(II) (1.2 mmol)	DMF/H ₂ O (3/3 ml), 80°C	7	95 ^[50]
4	Pd (1.0 mol)	K ₃ PO ₄ .3H ₂ O (1.5 mmol), H ₂ O/ethanol (2 ml), 80°C	3	98 ^[51]
5	Cross-linked poly(ITC-HPTPy)-Pd (0.23 mol%)	K ₂ CO ₃ (1.5 mmol), H ₂ O/ethanol (3 ml), 80°C	2	98 ^[52]
6	CuCl ₂ (10 mol%), 4,4'-di- <i>tert</i> -butyl-2,2'-bipyridine (10 mol%)	DCM (1.0 ml), Cs ₂ CO ₃ (2.0 equiv), r.t.	24	78 ^[53]
7	Hercynite@L-methionine-Pd (0.1 mol%)	K ₂ CO ₃ (3 mmol), ethanol (3 ml), 80°C	1.5	80 ^[54]
8	GO/Fe ₃ O ₄ /Pd nanocomposite (0.36 mol)	K ₂ CO ₃ (3 mmol), H ₂ O/ethanol (3 ml), 80°C	10	80 ^[55]
9	Cu(II)-β-cyclodextrin (0.1 eq)	DMF, 90°C	10	80 ^[56]
10	Cu-PAR (0.05 g, 0.0129 mmol)	KOH (1 mmol), DMSO, 120°C	14	94 ^[57]
11	Cu-BIA-Si-Fe ₃ O ₄ (1.5 mol%)	K ₂ CO ₃ (1 mmol), DMSO, 80°C	2	95 (present work)

^aYields refer to isolated pure products.

with both electron-withdrawing and electron-releasing groups reacted efficiently and afforded products in excellent yields.

A proposed mechanism for the reaction is shown in Scheme 3. First, the coupling of aromatic amines and boronic acids is as depicted in Scheme 1. The reaction is initiated by nucleophilic coordination of amine with Cu(II) of the Cu-BIA-Si-Fe₃O₄ catalyst resulting (A), which undergoes transmetalation with boronic acid to furnish coupled Cu(II) complex (B). Oxidation of (B) in turn affords complex (C) involving Cu as Cu(III). Complex (C) on reductive elimination furnishes the final C&—N coupled product (D) and regenerates Cu(I) catalyst which is further oxidized to Cu(II) in the presence of air. There is an added advantage of the magnetically separable heterogeneous catalyst in that it can be easily recovered after completion of the reaction without any significant loss (Scheme 3).

To investigate the activity and efficiency of the catalyst in comparison with catalysts reported in the literature for the synthesis of diphenylamine derivatives, the reaction of boronic acid with aniline was evaluated as a representative example and conducted in the presence of different catalysts. The results exhibited that these methods are comparable to some previously reported methods in terms of reaction times and yields (Table 6).

The recoverability and reusability of the prepared catalyst were studied using the selected model reaction of

aniline and phenylboronic acid in DMSO (Table 5, entry 1). The results demonstrated that Cu-BIA-Si-Fe₃O₄ is a sustainable catalyst in reaction media and can be reused four times with no significant loss of its catalytic activity (Figure 9).

The recycled Cu-BIA-Si-Fe₃O₄ catalyst (after four recycles) was characterized using FT-IR spectroscopy, SEM, EDX analysis, TGA and TEM, as shown in Figures 10–14.

The FT-IR spectrum of recovered Cu-BIA-Si-Fe₃O₄ is illustrated in Figure 10. The peaks at around 2930 and 2852 cm⁻¹, for asymmetric and symmetric vibrations of C&—H stretching, can be obviously observed. The absorption peaks at 1630 and 1450 cm⁻¹ correspond to the asymmetric and symmetric stretching vibration of C&=N and C&—H (aromatic) of organic moiety. The absorption bands at 586 and 447 cm⁻¹ were attributed to Fe&—O stretching and that at 3443 cm⁻¹ corresponded to OH groups on magnetic surface of Fe₃O₄. Therefore, the data obtained from FT-IR spectroscopy indicate the existence of the nanomagnetic particles, heterocyclic moiety and Cu in the structure of Cu-BIA-Si-Fe₃O₄ MNPs (Figure 10).

Morphologies of recovered Cu-BIA-Si-Fe₃O₄ nanoparticles were investigated using TEM as shown in Figure 11. Particles are observed to have spherical morphology. Average particle size is estimated at about 14 nm from the TEM micrographs. Also, an SEM image of the recovered Cu-BIA-Si-Fe₃O₄ nanoparticles is shown

TABLE 4 Optimization of reaction conditions for synthesis of diarylamine

Entry	Solvent	Amount of catalyst (mol%)	Base	Temperature (°C)	Time (h)	Yield (%) ^[a]	TON	TOF (h ⁻¹)
1	CH ₃ CN	2	KF (1 mmol)	70	10	70	35	3.5
2	DMF	2	KF (1 mmol)	110	4	75	37.5	9.37
3	DMSO	2	KF (1 mmol)	100	2.5	97	48.5	19.4
4	CH ₃ OH	2	KF (1 mmol)	60	10	65	32.5	3.25
5	H ₂ O	2	KF (1 mmol)	100	12	40	20	1.66
6	DMSO	1.5	KF (1 mmol)	100	2.5	97	64.6	25.84
7	DMSO	1.5	DABCO (1 mmol)	100	3	75	50	16.66
8	DMSO	1.5	Et ₃ N (1 mmol)	100	2.5	82	54.6	21.84
9	DMSO	1.5	NaOH (1 mmol)	100	2.5	79	52.6	21.04
10	DMSO	0.5	KF (1 mmol)	75	5	20	40	8
11	DMSO	1	KF (1 mmol)	75	5	40	40	8
12	DMSO	1.5	KF (1 mmol)	75	5	65	43.3	8.66
13	DMSO	2	KF (1 mmol)	75	4.5	75	37.5	8.33
14	DMSO	0.5	KF (1 mmol)	100	3	65	130	43.33
15	DMSO	1	KF (1 mmol)	100	3	85	85	28.33
16	DMSO	1.5	KF (1 mmol)	100	2.5	97	64.6	25.84
17	DMSO	2	KF (1 mmol)	100	2.5	97	64.6	25.84
18	DMSO	1.5	KF (0.5 mmol)	100	2.5	96	64	25.6
19	DMSO	1.5	KF (0.2 mmol)	100	2.5	96	64	25.6
20	No catalyst	2	KF (1 mmol)	100	24	No reaction	—	—
21	CuCl ₂ –DMSO	2	KF (1 mmol)	100	4	78	39	9.75

^aYields refer to isolated products.

in Figure 12. The SEM image of Cu-BIA-Si-Fe₃O₄ showed a sphere-like structure.

The TGA curve of the recovered nanoparticles shows the mass loss of the organic functional group as it decomposes upon heating. The curve shows a weight loss of about 13.4% from 680°C, resulting from the decomposition of functional groups grafted to the MNP surface (Figure 13).

As can be seen from the FT-IR analysis, the structure of the Cu-BIA-Si-Fe₃O₄ catalyst has not changed and, according to SEM analysis, the catalyst particles are spherical. Also, the size of the recycled catalyst particles is similar to those of the newly synthesized particles from the TEM analysis, and EDX analysis has also not changed (Figure 14). Therefore, based on the obtained results, the Cu-BIA-Si-Fe₃O₄ catalyst has not changed after four recycles and its activity is similar to that of the newly prepared catalyst.

The results demonstrated that the Cu-BIA-Si-Fe₃O₄ catalyst could be reused four times without losing its

efficiency. It should be noted that there was low Cu leaching (about 9.7%) during the reaction and the catalyst showed high stability even after four cycles.

3 | EXPERIMENTAL

3.1 | Chemicals and apparatus

Powder XRD of the prepared catalyst was performed using a Philips PW 1830 X-ray diffractometer with a Cu K α source ($\lambda = 1.5418 \text{ \AA}$) in the Bragg angle range 10–80° at 25°C. FT-IR spectra were obtained using a FT-IR spectrometer (Vector 22, Bruker) in the range 400–4,000 cm⁻¹ at room temperature. SEM analysis was conducted using a VEGA//TESCAN KYKY-EM 3200 microscope (acceleration voltage of 26 kV). TEM experiments were conducted with a Philips EM 208 electron microscope. EDX analysis of the catalyst was conducted with a VEGA3 XUM/TESCAN. TGA was performed with a Stanton Red

TABLE 5 Synthesis of diarylamines in the presence of Cu-BIA-Si-Fe₃O₄ as catalyst

Entry	Boronic acid	Aniline	Time (h)	Yield (%) ^[a]	TON (%)	Melting point (°C)	
						Found	Reported
1			2.5	96	64	53–54	52–54 ^[58]
2			2	97	64.6	64–66	65–66 ^[11]
3			2.5	95	63.3	91–92	90 ^[8]
4			2.5	95	63.3	84–85	85–87 ^[58]
5			2	98	65.3	137	135–136 ^[8]
6			2.5	95	63.3	136–137	135–136 ^[8]
7			2	96	64	80–82	81–83 ^[59]
8			2	95	63.3	136–137	135–137 ^[60]
9			2.5	97	64.6	91–92	90 ^[8]

TABLE 5 (Continued)

Entry	Boronic acid	Aniline	Time (h)	Yield (%) ^[a]	TON (%)	Melting point (°C)	
						Found	Reported
10			2	98	65.3	72–74	73–75 ^[58]
11			2.5	95	63.3	79–80	80–81 ^[8]

^aYields refer to the isolated products.

SCHEME 3 Suggested mechanism for *N*-arylation reactions in presence of Cu-BIA-Si-Fe₃O₄ nanocatalyst

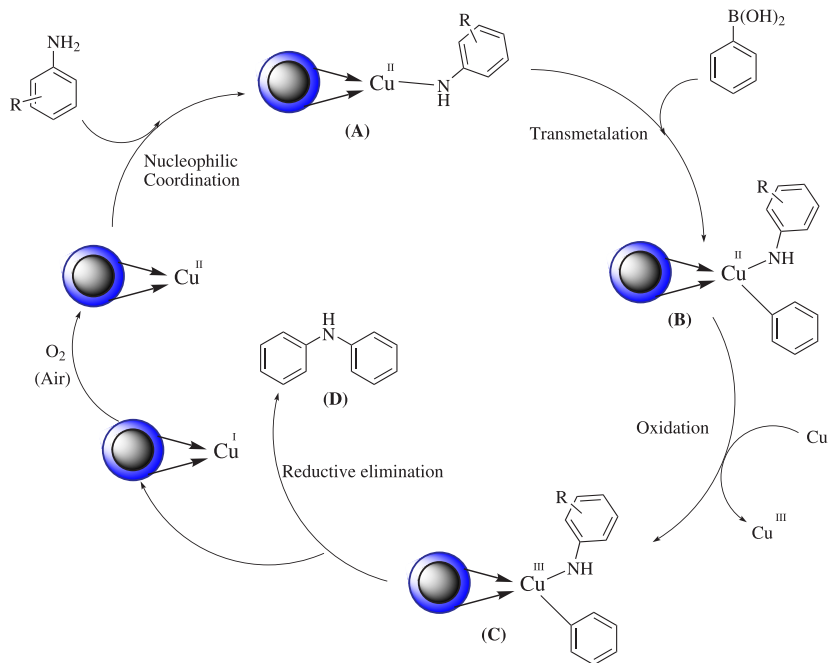


TABLE 6 Comparison of results for present catalyst with those for other reported catalysts in the synthesis of diphenylamine

Entry	Catalyst	Conditions	Time (h)	Yield (%) ^[a]
1	Cu ₂ -β-CD (0.01 mmol), K ₂ CO ₃ (3 equiv.)	DMF (1 ml), 90°C	48	90 ^[61]
2	Cu(OAc) ₂ (5–20 mol %), myristic acid (10–40 mol%)	Toluene (2 ml), r.t.	24	92 ^[62]
3	CuFAP (100 mg)	Methanol (4 ml), r.t.	3	90 ^[63]
4	Cu-BIA-Si-Fe ₃ O ₄ (1.5 mol%), KF (0.2 mmol)	DMSO (4 ml), 100°C	2.5	96 (present work)

^aIsolated yield.

Craft STA-780 (London, UK). NMR spectra were performed with a Bruker DRX-400 AVANCE instrument (300.1 MHz for ¹H, 75.4 MHz for ¹³C). The spectra were obtained with samples in DMSO-*d*₆ as a solvent.

Magnetic measurements were carried out using a VSM instrument (MDK, model 7400). The metal loading was determined using ICP-AES. Melting points were evaluated with an Electrothermal 9100 apparatus.

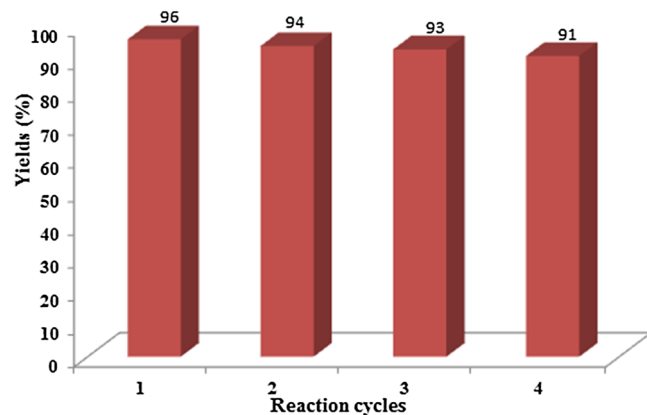


FIGURE 9 Reusability of the catalyst

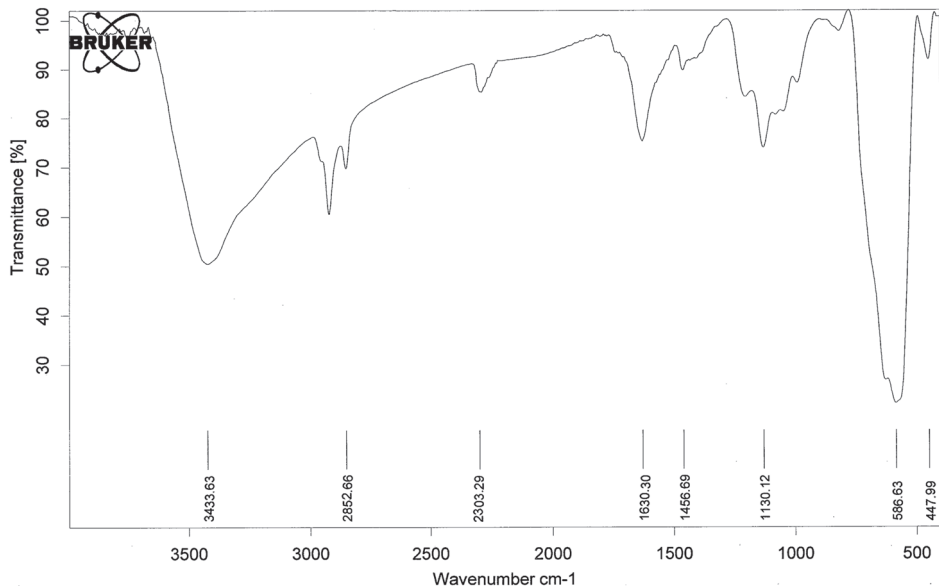


FIGURE 10 FT-IR spectrum of Cu-BIA-Si-Fe₃O₄ nanoparticles after four recycles

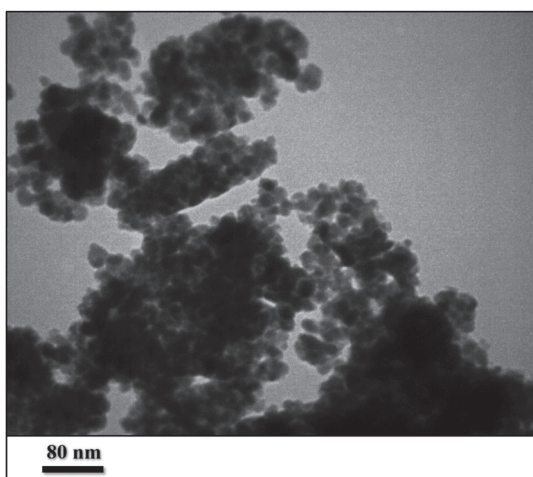


FIGURE 11 TEM analysis of Cu-BIA-Si-Fe₃O₄ nanoparticles after four recycles

3.2 | General procedures

3.2.1 | Preparation of Fe₃O₄ MNPs

FeCl₃·6H₂O (2 mol) and FeCl₂·4H₂O (1 mol) were added to 100 ml of deionized water and then sonicated to dissolve all salts entirely. Afterwards, 10 ml of 25% NH₄OH was added quickly into the reaction mixture in one portion under nitrogen atmosphere at room temperature followed by vigorous stirring for about 25 min with a magnetic stirrer. The black precipitate was washed with deionized water four times (Scheme 4).

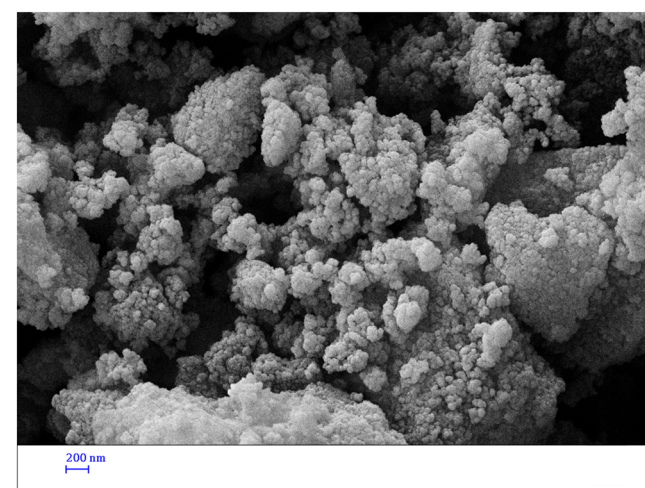


FIGURE 12 SEM analysis of Cu-BIA-Si-Fe₃O₄ nanoparticles after four recycles

FIGURE 13 TGA of Cu-BIA-Si- Fe_3O_4 nanoparticles after four recycles

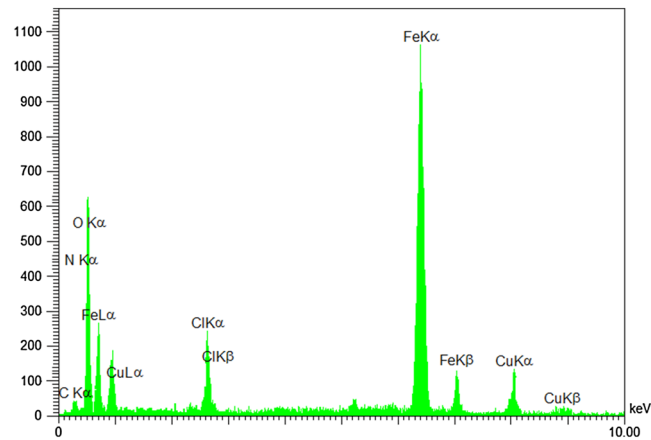
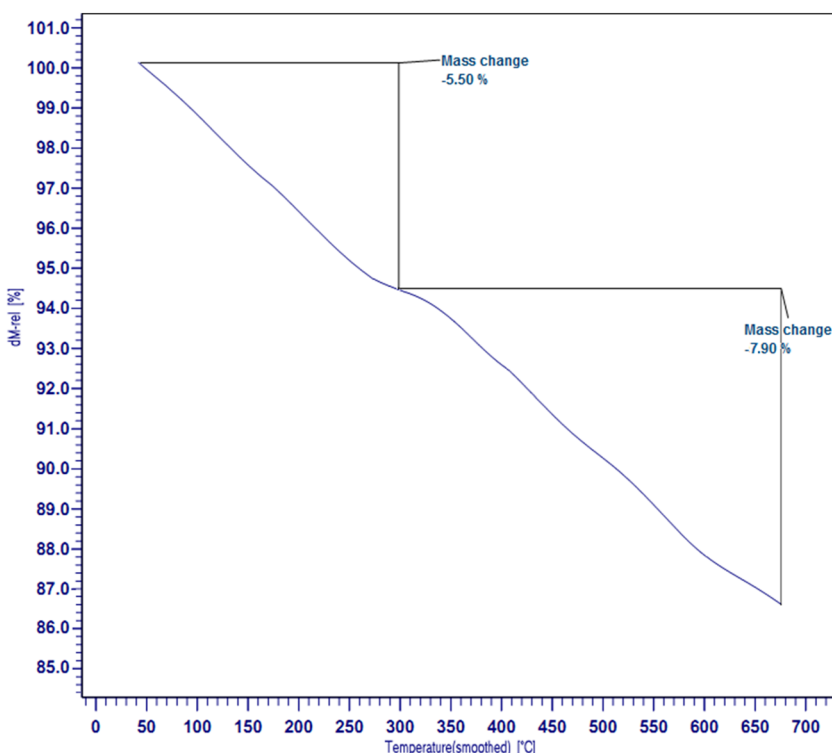
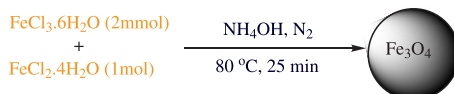


FIGURE 14 EDX analysis of Cu-BIA-Si- Fe_3O_4 nanoparticles after four recycles

3.2.2 | Preparation of 3-chloropropyltrimethoxysilane-functionalized Fe_3O_4 nanoparticles ($\text{Fe}_3\text{O}_4\text{-ClPSi}$)

Initially, 1.5 g of Fe_3O_4 MNPs was added to 100 ml of ethanol and placed in an ultrasonic apparatus for 25 min.

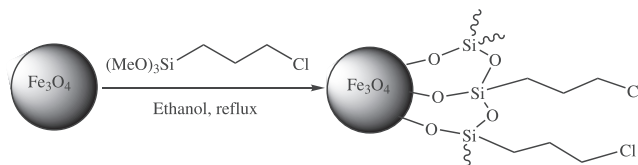


SCHEME 4 Preparation of Fe_3O_4 nanoparticles

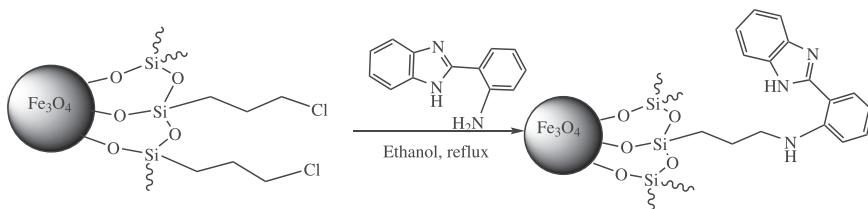
After that, 2.5 ml of 3-chloropropyltrimethoxysilane was added under reflux condition and stirred for 3.5 h with a mechanical stirrer. The obtained precipitate was filtered off with an external magnet and washed twice with ethanol and dried overnight in an oven at 85°C to afford Fe_3O_4 nanoparticles coated with 3-chloropropyltriethoxysilane (Scheme 5).

3.2.3 | Preparation of BIA-Si- Fe_3O_4 nanoparticles

First, 1.5 g of Fe_3O_4 nanoparticles was added to 150 ml of ethanol and placed in an ultrasonic apparatus for 30 min. Then 1 g of 1*H*-benzo[*d*]imidazol-2-amine was added under reflux conditions and stirred vigorously with a mechanical stirrer for 8 h. The obtained precipitate was filtered off with an external magnet, rinsed with ethanol several times and placed in an oven for 24 h to dry to afford the product of 1*H*-benzo[*d*]imidazol-2-amine-coated iron oxide nanoparticles (Scheme 6).



SCHEME 5 Preparation of $\text{Fe}_3\text{O}_4\text{-ClPSi}$ nanoparticles



S C H E M E 6 Preparation of BIA-Si- Fe_3O_4 nanoparticles

3.2.4 | Preparation of Cu-BIA-Si- Fe_3O_4 nanoparticles

To prepare Cu-BIA-Si- Fe_3O_4 nanoparticles, the obtained BIA-Si- Fe_3O_4 (0.5 g) was dispersed in 50 ml of ethanol by sonication for 30 min, and then 0.045 g of CuCl_2 was added to the mixture. A brown suspension was formed after refluxing with vigorous stirring for 8 h. The catalyst (Cu-BIA-Si- Fe_3O_4) was separated from the solution using an external magnet, washed with deionized water several times and dried in an oven overnight (Scheme 7). The whole synthesis was performed under nitrogen flow.

3.2.5 | General procedure for synthesis of diaryls via Suzuki coupling reactions

To synthesize diaryls via Suzuki coupling reactions, aryl halide (1 mmol), phenylboronic acid (1 mmol) and 1 mmol of K_2CO_3 as the base were mixed with each other in DMSO (2.5 ml) in the presence of Cu-BIA-Si- Fe_3O_4 (1.5 mol%) as catalyst. The reaction mixture was stirred vigorously at 80°C for various times according to each substrate. After reaction, the solid catalyst was filtered and washed several times with deionized water and absolute ether and kept for reuse in a subsequent run under the same reaction conditions. The filtrate was extracted with ethyl acetate (3×5 ml), washed with deionized water, dried with anhydrous MgSO_4 , filtered and the solvent was evaporated and the final product purified and prepared by preparative TLC (eluent: petroleum ether–ethyl acetate, 20/1) and the obtained product yield evaluated.

Two known and reported synthesized compounds are described with their characterization data below:

4-Methoxybiphenyl (Table 2, entry 1): ^1H NMR (400 MHz, $\text{DMSO}-d_6$, δ , ppm): 3.61 (s, 3H, OCH_3), 6.90

(d, $J = 8.8$ Hz, 2 H_{Ar}), 7.01 (d, $J = 8.8$ Hz, 2 H_{Ar}), 7.19–7.31 (m, 4 H_{Ar}). ^{13}C NMR (100 MHz, $\text{DMSO}-d_6$, δ , ppm): 54.8, 119.2, 126.0, 127.7, 129.4, 129.6, 131.4, 139.9, 159.7.

4-Methoxy-4'-ethylbiphenyl (Table 2, entry 3): ^1H NMR (400 MHz, $\text{DMSO}-d_6$, δ , ppm): 1.20 (t, $J = 8.4$ Hz, 3 H_{CH_3}), 2.27 (q, $J = 8.4$ Hz, 2H CH_2), 3.61 (s, 3H, OCH_3), 6.81–6.85 (m, 2 H_{Ar}), 6.94–7.00 (m, 2 H_{Ar}), 7.07–7.11 (m, 4 H_{Ar}). ^{13}C NMR (100 MHz, $\text{DMSO}-d_6$, δ , ppm): 18.8, 28.4, 51.8, 118.0, 123.6, 123.7, 126.4, 126.5, 130.5, 134.4, 160.0.

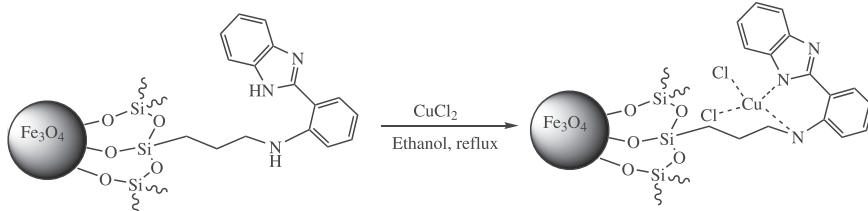
3.2.6 | General procedure for *N*-arylation reactions

A mixture of phenylboronic acid (1 mmol), aromatic amine (1.2 mmol) and 0.12 g (0.2 mmol) of KF in DMSO (4 ml) was added to Cu-BIA-Si- Fe_3O_4 (1.5 mol%) under nitrogen atmosphere at 100°C for 2 h with vigorous stirring. Then, after completion of the reaction, the catalyst was separated using an external magnet and washed with dry CH_2Cl_2 three times and checked for its reusability. The solvent of the reaction mixture was evaporated using a rotary evaporator and then ethyl acetate and water were added to the residue. The organic layer was dried over anhydrous MgSO_4 . The solvent was evaporated under reduced pressure and the crude product was purified by column chromatography using ethyl acetate–*n*-hexane.

Selected spectral data for a two known products are given below:

Diphenylamine (Table 5, entry 1): ^1H NMR (400.13 MHz, DMSO, δ , ppm): 5.60 (s, 1H, N-H), 7.12–1.15 (m, 2 H_{Ar}), 7.22–7.27 (m, 4 H_{Ar}) ppm, 7.38 (d, 4 H_{Ar}). ^{13}C NMR (100.6 MHz, DMSO, δ , ppm): 119.9, 121.0, 123.7, 136.3.

4-Methyl-*N*-phenylaniline (Table 5, entry 3): ^1H NMR (400.13 MHz, DMSO, δ , ppm): 2.30 (s, 3H, CH_3), 5.60 (s, 1H, N–H), 7.09–7.20 (m, 2H), 7.21–7.27 (m, 3H), 7.42



S C H E M E 7 Preparation of Cu-BIA-Si- Fe_3O_4 nanoparticles

(d, $J = 2.0$ Hz, 2H), 7.56 (d, $J = 2.0$ Hz, 2H). ^{13}C NMR (100.6 MHz, DMSO, δ , ppm): 19.0, 122.2, 123.0, 123.7, 123.9, 127.4, 131.5, 135.3, 135.9.

4 | CONCLUSIONS

A new and efficient catalyst consisting of copper supported on 2-(1*H*-benzo[*d*]imidazol-2-yl)aniline-functionalized Fe_3O_4 nanoparticles ($\text{Cu-BIA-Si-Fe}_3\text{O}_4$) has been developed as a highly active, stable and recoverable heterogeneous catalyst for the preparations of diaryl and diarylamines via Suzuki C&—C reactions and Ullmann coupling reactions between aryl halides with phenylboronic acid and boronic acid with aniline derivatives. The catalyst could be reused for several sequential cycles with no effective loss of its activity.

ACKNOWLEDGMENTS

The author acknowledges the Beijing, Tianjin and Hebei Governments under the Background of Service-oriented Government Construction for support of this work.

ORCID

Majid Mohammadnia  <https://orcid.org/0000-0001-8172-8244>

REFERENCES

- [1] F. Takehisa, M. Kenji, O. Satoshi, A. Hiroya, N. Makio, N. Kiyoshi, *J. Power Sources* **2004**, *125*, 17.
- [2] P. Barbaro, F. Liguori, Heterogenized homogeneous catalysts for fine chemicals production: materials and processes, Springer Science & Business Media, **2010**, 33.
- [3] D. Wang, D. Astruc, *Chem. Rev.* **2014**, *114*, 6949.
- [4] R. N. Baig, M. N. Nadagouda, R. S. Varma, *Coord. Chem. Rev.* **2015**, *287*, 137.
- [5] S. Asghari, M. Mohammadnia, *Inorg. Nano-Met. Chem.* **2017**, *47*, 1004.
- [6] M. Nasrollahzadeh, M. Maham, A. Rostami-Vartooni, M. Bagherzadeh, S. M. Sajadi, *RSC Adv.* **2015**, *5*, 64769.
- [7] S. Asghari, M. Mohammadnia, *Res. Chem. Intermed.* **2017**, *43*, 7193.
- [8] A. Ghorbani-Choghamarani, Z. Taherinia, *New J. Chem.* **2017**, *41*, 9414.
- [9] M. Shariatipour, A. Salamatmanesh, M. J. Nejad, A. Heydari, *Catal. Commun.* **2020**, *135*, 105890.
- [10] A. S. Guram, S. L. Buchwald, *J. Am. Chem. Soc.* **1994**, *116*, 7901.
- [11] J. C. Vantourout, R. P. Law, A. Isidro-Llobet, S. J. Atkinson, A. J. Watson, *J. Org. Chem.* **2016**, *81*, 3942.
- [12] V. Sadhasivam, B. Sankar, G. Elamathi, M. Mariyappan, A. Siva, *Res. Chem. Intermed.* **2020**, *46*, 681.
- [13] X. Zhang, F. Liu, Z. Wei, Z. Wang, *Lett. Org. Chem.* **2013**, *10*, 31.
- [14] N. Iranpoor, H. Firouzabadi, A. Rostami, *Appl. Organometal. Chem.* **2013**, *27*, 501.
- [15] K. C. Nicolaou, S. Natarajan, H. Li, N. F. Jain, R. Huges, M. E. Solomon, J. M. Ramanujulu, C. N. C. Boddy, *Angew. Chem. Int. Ed.* **1998**, *37*, 2708.
- [16] Q. Hang, D. P. Wang, X. Y. Wang, K. Ding, *J. Org. Chem.* **2009**, *74*, 7187.
- [17] G. Evano, N. Blanchard, M. Toumi, *Chem. Rev.* **2008**, *108*, 3054.
- [18] A. Y. Cheng, J. C. Hsieh, *Tetrahedron Lett.* **2012**, *53*, 71.
- [19] J. Lindley, *Tetrahedron* **1984**, *40*, 1433.
- [20] J. C. Henrim, P. C. Pascal, H. Samy, F. S. Jean, T. A. Marc, *Org. Lett.* **2004**, *6*, 913.
- [21] J. K. Huang, Y. Chen, J. H. Chan, L. R. Mike, D. L. Robert, M. F. Margaret, *Synlett* **2011**, *10*, 1419.
- [22] A. Shafir, P. A. Lichtor, S. L. Buchwald, *J. Am. Chem. Soc.* **2007**, *129*, 3490.
- [23] E. Buck, Z. J. Song, D. Tschaen, P. G. Dormer, R. P. Volante, P. J. Reider, *Org. Lett.* **2002**, *4*, 1623.
- [24] R. Zhang, J. Liu, S. Wang, J. Niu, C. Xia, W. Sun, *ChemCatChem* **2011**, *3*, 146.
- [25] S. V. Ley, A. W. Thomas, *Angew. Chem.* **2003**, *42*, 5400.
- [26] R. K. Gujadhur, C. G. Bates, D. Venkataraman, *Org. Lett.* **2001**, *3*, 4315.
- [27] F. Y. Kwong, A. Klapars, S. L. Buchwald, *Org. Lett.* **2002**, *4*, 581.
- [28] D. Ma, Q. Cai, *Org. Lett.* **2003**, *5*, 3799.
- [29] H. J. Cristau, P. P. Cellier, S. Hamada, J. F. Spindler, M. Taillefer, *Org. Lett.* **2004**, *6*, 913.
- [30] X. Lv, Z. Wang, W. Bao, *Tetrahedron* **2006**, *62*, 4756.
- [31] S. Zhang, D. Zhang, L. S. Liebeskind, *J. Org. Chem.* **1997**, *62*, 2312.
- [32] H. Rao, Y. Jin, H. Fu, Y. Jiang, Y. Zhao, *Eur. J. Dermatol.* **2006**, *12*, 3636.
- [33] P. J. Fagan, E. Hauptman, R. Shapiro, A. Casalnuovo, *J. Am. Chem. Soc.* **2000**, *122*, 5043.
- [34] A. A. Kelkar, N. M. Patil, R. V. Chaudhari, *Tetrahedron Lett.* **2002**, *43*, 7143.
- [35] Y. X. Xie, S. F. Pi, J. Wang, D. L. Yin, J. H. Li, *J. Org. Chem.* **2006**, *71*, 8324.
- [36] L. Liu, M. Frohn, N. Xi, C. Dominguez, R. Hungate, P. J. Reider, *J. Org. Chem.* **2005**, *70*, 10135.
- [37] E. Buck, Z. J. Song, D. Tschaen, P. G. Dormer, R. P. Volante, *J. Org. Lett.* **2002**, *4*, 1623.
- [38] C. Palomo, M. Oiarbide, R. López, E. Gómez-Bengoa, *Chem. Commun.* **1998**, *19*, 2091.
- [39] M. A. Zolfogol, V. Khakyzadeh, A. R. Moosavi-Zare, A. Rostami, A. Zare, N. Iranpoor, R. Luque, *Green Chem.* **2013**, *15*, 2132.
- [40] A. Shaabani, S. E. Afshari, R. Hooshmand, A. T. Tabatabaei, F. Hajishaabanha, *RSC Adv.* **2016**, *6*, 18113.
- [41] M. Waheed, N. Ahmed, *Synthesis* **2017**, *49*, 4372.
- [42] R. Rahil, S. Sengmany, E. Le Gall, E. Leonel, *Synthesis* **2018**, *50*, 146.
- [43] M. Planellas, R. Pleixats, A. Shafir, *Adv. Synth. Catal.* **2012**, *354*, 651.
- [44] J. M. Hammann, F. H. Lutter, D. Haas, P. Knochel, *Angew. Chem.* **2017**, *129*, 1102.
- [45] D. Qiu, H. Meng, L. Jin, S. Wang, S. Tang, X. Wang, F. Mo, Y. Zhang, J. Wang, *Angew. Chem. Int. Ed.* **2013**, *52*, 11581.
- [46] S. Ren, J. Zhang, J. Zhang, H. Wang, W. Zhang, Y. Liu, M. Liu, *Eur. J. Org. Chem.* **2015**, *2015*, 5381.

- [47] J. Tang, A. Biafora, L. J. Goossen, *Angew. Chem. Int. Ed.* **2015**, *54*, 13130.
- [48] F. Rajabi, W. R. Thiel, *Adv. Synth. Catal.* **2014**, *356*, 1873.
- [49] S. Yaşar, S. Çekirdek, İ. Özdemir, *Heteroatom Chem.* **2014**, *25*, 157.
- [50] M. Keleş, M. K. Yılmaz, *Appl. Organometal. Chem.* **2014**, *28*, 91.
- [51] B. Li, Z. Guan, W. Wang, X. Yang, J. Hu, B. Tan, T. Li, *Adv. Mater.* **2012**, *24*, 3390.
- [52] H. Targhan, A. Hassanpour, S. Sohrabnezhad, K. Bahrami, *Catal. Lett.* **2020**, *150*, 660.
- [53] Z. Zhu, J. Liu, S. Dong, B. Chen, Z. Wang, R. Y. Tang, Z. Li, *Asian J. Org. Chem.* **2020**, *9*, 631. <https://doi.org/10.1002/ajoc.202000007>
- [54] M. Mohammadi, A. Ghorbani-Choghamarani, *New J. Chem.* **2020**, *44*, 2919.
- [55] N. Seyedi, K. Saidi, H. Sheibani, *Catal. Lett.* **2018**, *148*, 277.
- [56] B. Kaboudin, Y. Abedi, T. Yokomatsu, *Eur. J. Org. Chem.* **2011**, *2011*, 6656.
- [57] M. Islam, S. Mondal, P. Mondal, A. S. Roy, K. Tuhina, M. Mobarok, S. Paul, N. Salam, D. Hossain, *Catal. Lett.* **2011**, *141*, 1171.
- [58] R. Singh, B. K. Allam, D. S. Raghuvanshi, K. N. Singh, *Tetrahedron* **2013**, *69*, 1038.
- [59] L. Cai, X. Qian, W. Song, T. Liu, X. Tao, W. Li, X. Xie, *Tetrahedron* **2014**, *70*, 4754.
- [60] J. Liu, D. Yang, X. Yang, M. Nie, G. Wu, Z. Wang, P. Gong, *Bioorg. Med. Chem.* **2017**, *25*, 4475.
- [61] B. Kaboudin, Y. Abedi, T. Yokomatsu, *Eur. J. Org. Chem.* **2011**, *33*, 6656.
- [62] J. C. Antilla, S. L. Buchwald, *Org. Lett.* **2001**, *3*, 2077.
- [63] M. L. Kantam, G. T. Venkanna, C. Sridhar, B. Sreedhar, B. M. Choudary, *J. Org. Chem.* **2006**, *71*, 9522.

SUPPORTING INFORMATION

Additional supporting information may be found online in the Supporting Information section at the end of this article.

How to cite this article: Danqing L, Ming J, Li L, Mohammadnia M. Preparation and characterization of Cu supported on 2-(1*H*-benzo[*d*]imidazol-2-yl)aniline-functionalized Fe₃O₄ nanoparticles as a novel magnetic catalyst for Ullmann and Suzuki cross-coupling reactions. *Appl Organomet Chem.* 2020;e5820. <https://doi.org/10.1002/aoc.5820>